BIOGEOGRAPHIA
The Journal of Integrative Biogeography

Biogeographia – The Journal of Integrative Biogeography 2026, 41 (2): a075

https://doi.org/10.21426/B6.64592

Soil Bacterial Composition Varies with Distance and Elevation from Interstate-495 in Queens, New York, USA

Catalina GARCIA CANAS[1], Ghazwan QASIM HASAN[2], Igor IVANOVSKI[1,*]

[1] *Department of Biology, St. Joseph's University, Patchogue, NY 11772, USA*
[2] *Department of Biology, University of Mosul, Mosul, Iraq*

corresponding author, email: iivanovski@sjny.edu

Keywords: *Achromobacter, Coxiella burnetii*, *Myxococcus*, Phylogenetics, Roadside.

SUMMARY

This study investigates how proximity and elevation relative to Interstate-495 highway (I-495) in Queens, New York, influence soil bacterial community structure. Twelve soil samples were collected across a 673,312-m² area with uniform sand, clay, and silt composition, spanning a gradient of increasing distance and elevation from roadside conditions (RC). Using 16S rRNA gene sequencing targeting the V3/V4 hypervariable regions, microbial diversity and composition were assessed across samples. Results revealed that soils closest to RC but at higher elevation exhibited reduced bacterial diversity and phylogenetic breadth, with dominance of *Coxiella burnetii*, *Streptococcus* spp., and *Achromobacter*. In contrast, the sample at the same elevation as the roadside (CC_I495_3) displayed the highest Shannon diversity (7.67), Faith's Phylogenetic Diversity (27.14), and a more even taxonomic distribution, including rare and evolutionarily distinct taxa such as *Myxococcus* and *Nitrospira*. Notably, uncultured species were significantly more prevalent in this low-elevation RC-exposed sample. Of the 502 operational taxonomic units (OTUs) identified, 189 were unique to RC-exposed soils, 114 were exclusive to NO-RC soils, and 199 were shared across both groups. These findings suggest that both proximity and elevation modulate microbial community assembly.

INTRODUCTION

Roadside soil is not conventionally regarded as a primary source for the isolation of high-efficiency hydrocarbon-degrading microorganisms, unlike soils contaminated by oil spills or other ecological disasters. Sites affected by significant petroleum contamination have been extensively studied due to their ability to support specialized microbial populations capable of hydrocarbon degradation (Atlas, 1981; Leahy & Colwell, 1990). In contrast, roadside environments accumulate pollutants through chronic, low-intensity exposure to vehicle emissions and construction activities, leading to gradual contamination over time (Bessagnet *et al.*, 2022; Lotfalian & Nasiri, 2018).

Vehicle exhaust composition varies based on fuel type, particularly between gasoline and diesel engines. Despite these differences, certain particulates remain consistently present in emissions, including aromatic and long-chain hydrocarbons,

carbon monoxide, and nitrogen oxides (Anigilaje *et al.*, 2024; Yang *et al.*, 2019). Roadside soils often exhibit elevated concentrations of heavy metals such as cadmium, cobalt, copper, lead, antimony, tin, and zinc, as documented in previous studies (Kaur *et al.*, 2022; Žibret *et al.*, 2013). While hydrocarbon contamination from roadside conditions is a recognized environmental factor, microbial communities in these soils have not traditionally been explored for their biodegradation potential in the same manner as highly contaminated industrial sites.

Hydrocarbon contamination leads to notable shifts in bacterial composition compared to uncontaminated soil environments (Melekhina *et al.*, 2021). These altered microbial communities frequently support the isolation of high-efficiency hydrocarbon-degrading strains, which contribute significantly to the biodegradation of pollutants (Y. Q. Li *et al.*, 2023). Several physicochemical factors influence microbial assemblages, including soil organic carbon content, total nitrogen availability, and heavy metal concentrations—such as cadmium, chromium, zinc, and copper (He *et al.*, 2020). Notably, roadside soils polluted with heavy metals tend to exhibit a higher prevalence of *Bacillus* species (Singh & Hiranmai, 2021). Comparative analyses indicate that *Bacillus*, along with *Gemmatimonas*, *Terrimonas*, and *Nitrospira*, demonstrates greater tolerance to roadside conditions, whereas *Barnesiella* and *Blastococcus* are more sensitive to environmental fluctuations near highways (Liu *et al.*, 2021).

Several cemeteries on Long Island, New York, have been examined for their soil microbiomes, revealing distinct microbial compositions predominantly composed of Proteobacteria, Planctomycetes, Bacteroidetes, Actinobacteria, Chloroflexi, Verrucomicrobia, and Acidobacteria (Caputo *et al.*, 2019). Calvary Cemetery, situated in Queens, New York, has been in operation since 1848 and is widely recognized for its cultural significance, having been featured in Mario Puzo's film *The Godfather* (1974). The cemetery's proximity to Interstate-495, which was expanded adjacent to the burial site in 1962, has resulted in sustained exposure to vehicular traffic. Currently, approximately 120,000 vehicles traverse the Long Island section of Queens daily (Transportation, 2019).

In this study, soil samples collected from Calvary Cemetery are analyzed with attention to maintaining consistent sand, clay, and silt composition. The investigation focuses on determining the extent to which roadside conditions influence microbial community structure within these soil environments. By examining bacterial populations in samples that vary in proximity and elevation relative to roadside exposure, the study aims to clarify how vehicular emissions and associated pollutants affect microbial diversity and community dynamics.

MATERIALS AND METHODS

Sample Collection

The geospatial analysis of Calvary Cemetery (Figure 1) was conducted using Google Earth version 7.3.6 for Windows, www.google.com/earth (Mountain View, CA, USA). The latitude, longitude and elevation of the sampling locations are listed in (Table 1). Samples were taken from four inches deep using a sterile stainless steel handheld auger sampler. Soil samples were observed on a compound light microscope to confirm that all the samples were of identical composition. The samples were collected on March 3rd, 2024. DNA was isolated using the QIAGEN DNeasy Powersoil Pro kit (Germantown, MD, USA) using the manufacturers guidelines.

16S rRNA Sequencing

The V3/V4 region of the 16S rRNA gene was sequenced using two forward primers (CCTACGGGDGGCWGCAG and CCTAYGGGGYGCWGCAG), and one reverse primer (GACTACHVGGGTATCTAATCC). SeqCenter (Pittsburgh, PA, USA) performed all 16S sequencing services and the reads were uploaded to the NCBI SRA database under accession number PRJNA1248142. Samples were sequenced on a P1 600cyc NextSeq2000 Flowcell to generate 2 x 301 base pairs (bp) paired end reads. Quality control and adapter trimming was performed with bcl-convert (bcl-convert). Sequences were imported into Qiime2 for subsequent analysis (Bolyen, 2019). Primer sequences were removed using Qiime2's cutadapt plugin (Martin, 2011). Sequences were denoised using Qiime2's dada2 plugin (Callahan *et al.*, 2016). Denoised sequences were assigned OTUs using the Silva 138 99% OTUs full-length sequence database and the VSEARCH (Torbjørn

Figure 1. Map of Calvary Cemetery. Sampling locations exposed to roadside conditions are marked in red and sampling locations with no roadside exposure are marked in blue.

Table 1. Sampling Locations and Corresponding Elevations, Referenced to the World Geodetic System 1984 (WGS84) Coordinate Framework.

Sample	Latitude	Longitude	Elevation from Roadside Conditions (RC)
CC_I495_1	40.73658337436522° N	-73.93107281269114° W	4.0 meters
CC_I495_2	40.73617690161965° N	-73.92862663823628° W	2.8 meters
CC_I495_3	40.73544524441922° N	-73.92574058153235° W	0.5 meters
CC_I495_4	40.73549402181626° N	-73.93183455999954° W	2.9 meters
CC_I495_5	40.73434774353139° N	-73.93008575984082° W	3.1 meters
CC_I495_6	40.73328274388058° N	-73.92798290811622° W	3.7 meters
CC_I495_7	40.73450220771404° N	-73.93350825831097° W	3.0 meters
CC_I495_8	40.73301445883763° N	-73.93203840787081° W	3.9 meters
CC_I495_9	40.73137220560313° N	-73.92962441992165° W	4.4 meters
CC_I495_10	40.73339656145070° N	-73.93607244995474° W	3.1 meters
CC_I495_11	40.73142911604667° N	-73.93365846200558° W	3.3 meters
CC_I495_12	40.72974857737732° N	-73.93106933172263° W	3.9 meters

Table 2. Sequencing Results.

Sample	Total Read Pairs	Total bp > Q30	% bp > Q30
CC_I495_1	17525	9167782	87.054
CC_I495_2	17130	8942342	86.881
CC_I495_3	41488	22139103	89.635
CC_I495_4	15071	7842732	86.83
CC_I495_5	21563	11334803	87.436
CC_I495_6	15395	8033581	86.806
CC_I495_7	18497	9697167	87.229
CC_I495_8	12776	6677928	86.97
CC_I495_9	23482	12343423	87.457
CC_I495_10	32198	16900921	87.339
CC_I495_11	37089	19600227	87.907
CC_I495_12	30293	15825237	86.916

Rognes *et al.*, 2016) utility within Qiime2's feature-classifier plugin. OTUs were then collapsed to their lowest taxonomic units, and their counts were converted to reflect their relative frequency within a sample. The complete list of OTUs generated with their relative frequency within the sample can be found in (Supplementary Material 1). The total read counts and their quality are listed in (Table 2).

Analysis and Evolutionary Relationships

The parts-of-whole figures were rendered using Qiime2's website https://view.qiime2.org/ and GraphPad Prism version 10.0.0 for Windows, www.graphpad.com (Boston, MA, USA). The beta diversity figures were rendered using Qiime2's website. Beta diversity was assessed using Bray-Curtis, Jaccard, Unweighted UniFrac, and Weighted UniFrac metrics to capture different aspects of microbial community variation. Bray-Curtis and Weighted UniFrac account for taxon abundance, while Jaccard and Unweighted UniFrac focus on community membership. UniFrac metrics additionally incorporate phylogenetic relationships. In each case, Principal Coordinates Analysis (PCoA) decomposes the distance matrix into orthogonal axes (Axis 1, Axis 2, Axis 3). Axis 3 represents the third principal coordinate derived from the same distance matrix and accounts for the least amount of variation in community dissimilarities, capturing additional structure that is not visible in the two-dimensional format of the figures.

For the heatmap, amplicon sequence variant counts were aggregated at the phylum level and normalized to relative abundance per sample by dividing each phylum's count by the total number of classified reads in that sample. The resulting proportions were used to construct a heatmap using the pheatmap package in R (v4.3.1). Samples were arranged by collection order, and taxa were ordered by overall abundance. Color intensity reflects normalized abundance, with darker shades indicating higher representation.

Sequences were aligned using the Clustal W multiple sequence alignment program (Larkin *et al.*, 2007). Evolutionary analyses, as well as rendering dendrograms, was conducted in MEGA11 (Tamura *et al.*, 2021). The evolutionary history was inferred using the Neighbor-Joining method (Saitou & Nei, 1987). The evolutionary distances were computed using the Maximum Composite Likelihood method (Tamura *et al.*, 2004) and are in the units of the number of base substitutions per site. Each analysis involved 21 nucleotide sequences. All codon positions were included and ambiguous positions were removed for each sequence pair using the pairwise deletion option. There was a total of 301 positions for each dataset.

RESULTS

Microbial Diversity

501 OTUs were generated across the 12 sampling locations, and the alpha diversity metrics can be seen in (Table 3). Samples CC_I495_1 and CC_I495_2, with RC exposure, showed to have the lowest average Shannon Diversity Index, Faiths Phylogenetic Diversity Index, and Pielou's Evenness Index. Conversely, Samples CC_I495_3 and CC_I495_7 exhibited the highest Shannon Diversity Index (7.67 and 5.07, respectively) and Faith's Phylogenetic Diversity (27.14 and 11.80), corresponding with broad representation of taxa such as *Coxiella burnetii*, *Streptococcus parasanguinis*, *Pseudomonas*, *Myxococcus*, and *Nitrospira*. These samples displayed balanced abundance profiles and high evenness, suggesting a stable and phylogenetically rich microbial community. In contrast, samples CC_I495_5 and CC_I495_8 showed reduced diversity and evenness, with dominance of fewer taxa including *Rubrobacter*, *Leuconostoc lactis*, and *Achromobacter*. These skewed profiles indicate potential niche specialization or environmental stress. Intermediate

samples (e.g., CC_I495_10, CC_I495_11, CC_I495_12) maintained moderate diversity and shared several core taxa with the high-diversity cluster, though with less phylogenetic breadth.

The Bray-Curtis Principal Coordinates Analysis (PCoA) plot (Figure 2) revealed two major clusters among the 12 soil samples, driven primarily by differences in taxon abundance. Samples CC_I495_3, CC_I495_7, CC_I495_10, CC_I495_11, and CC_I495_12 formed a distinct cluster, characterized by elevated Shannon diversity (mean ≈ 5.19) and higher Faith's Phylogenetic Diversity. These samples exhibited increased relative abundance of *Coxiella burnetii*, *Streptococcus parasanguinis*, and *Pseudomonas*, suggesting a more complex and even microbial community. In contrast, samples CC_I495_1, CC_I495_2, CC_I495_4, CC_I495_5, CC_I495_6, CC_I495_8, and CC_I495_9 were more dispersed, with lower evenness and dominance of *Streptococcus* spp., *Coxiella*, and *Achromobacter*. Notably, CC_I495_3 stood out with the highest Shannon index (7.67) and Faith's PD (27.14), indicating a highly diverse and phylogenetically rich community. The Bray-Curtis metric effectively captured abundance-driven shifts, highlighting the influence of dominant taxa in structuring microbial assemblages.

Table 3. Alpha Diversity.

Sample	Shannon Diversity Index	Faith's Phylogenetic Diversity	Pielou's Evenness
CC_I495_1	4.70130	9.04969	0.75476
CC_I495_2	4.65718	10.0825	0.74768
CC_I495_3	7.67433	27.1372	0.89872
CC_I495_4	4.69240	8.62173	0.74655
CC_I495_5	4.43301	8.72491	0.71391
CC_I495_6	4.51367	9.75532	0.73156
CC_I495_7	5.06577	11.8025	0.75294
CC_I495_8	4.13590	9.11868	0.67941
CC_I495_9	4.64817	10.4476	0.72143
CC_I495_10	5.00948	10.3585	0.74919
CC_I495_11	5.12138	9.63865	0.77773
CC_I495_12	5.06710	9.80914	0.76603

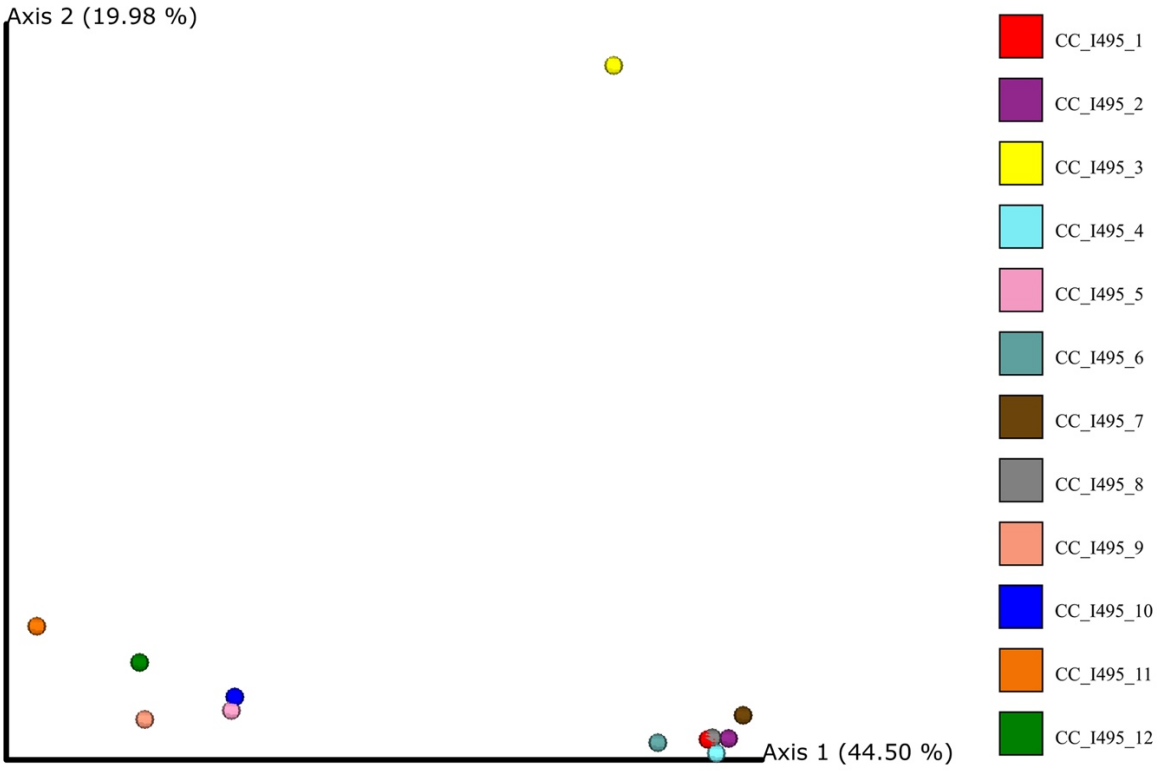

Figure 2. PCoA based on Bray-Curtis dissimilarity of 16S rRNA gene sequences across 12 soil samples. Axes 1 and 2 are shown in the figure; Axis 3 accounts for 12.59% of the variation in community dissimilarities.

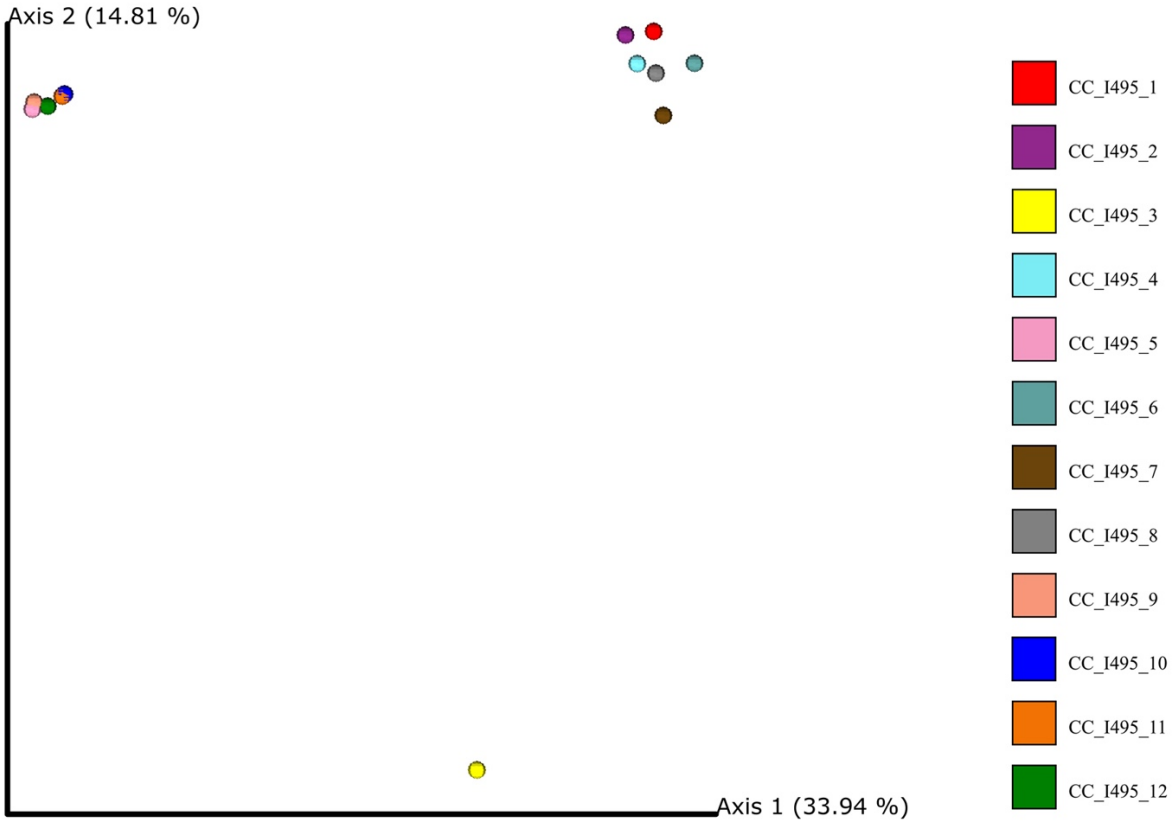

Figure 3. PCoA based on Jaccard index, emphasizing presence/absence of taxa across 12 soil samples. Axes 1 and 2 are shown in the figure; Axis 3 accounts for 8.16% of the variation in community dissimilarities.

The Jaccard-based PCoA plot (Figure 3), which emphasizes presence/absence rather than abundance, revealed more diffuse clustering. Samples CC_I495_3 and CC_I495_7 remained central, suggesting shared core taxa across groups. However, CC_I495_5 and CC_I495_8 appeared as outliers, driven by unique taxa such as *Lactococcus lactis*, *Rubrobacter*, and *Leuconostoc lactis*. These samples also had lower evenness and Shannon diversity, indicating a skewed community composition dominated by fewer taxa. The presence of rare but distinct OTUs in CC_I495_5 and CC_I495_8 contributed to their separation, underscoring the Jaccard metric's sensitivity to community membership turnover. Samples CC_I495_10 through CC_I495_12 clustered moderately, sharing taxa like *Pseudomonas*, *Streptococcus uberis*, and *Enterococcus faecalis*, but with subtle differences in rare taxa composition.

Unweighted UniFrac analysis (Figure 4), which incorporates phylogenetic relationships based on presence/absence, revealed pronounced separation of CC_I495_3 from all other samples. This sample harbored evolutionarily distinct taxa such as *Myxococcus*, *Nitrospira*, and *Skermanella*, contributing to its high Faith's PD and unique phylogenetic signature. CC_I495_5 and CC_I495_8 also diverged from the main cluster due to the presence of *Rubrobacter*, *Bifidobacterium*, and *Leuconostoc*, which are phylogenetically distant from the dominant taxa in other samples. Samples CC_I495_10, CC_I495_11, and CC_I495_12 clustered closely, reflecting shared phylogenetic structure despite moderate taxonomic overlap. The metric highlighted the role of rare, evolutionarily distinct taxa in shaping community dissimilarity.

Weighted UniFrac PCoA (Figure 5), which integrates both abundance and phylogeny, showed the most pronounced clustering. Samples CC_I495_3, CC_I495_7, CC_I495_10, CC_I495_11, and CC_I495_12 formed a tight group, driven by dominant and phylogenetically diverse taxa such as *Coxiella burnetii*, *Streptococcus parasanguinis*, *Pseudomonas*,

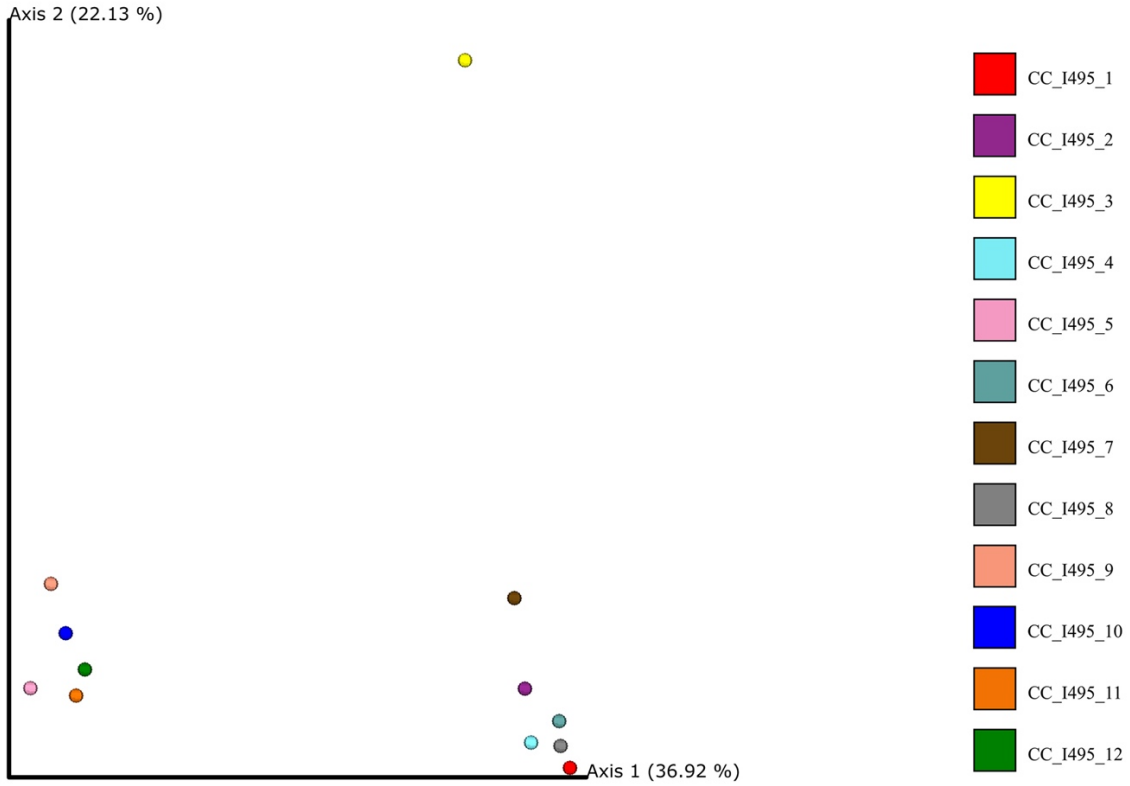

Figure 4. PCoA derived from Unweighted UniFrac distances, incorporating phylogenetic relationships based on presence/absence across 12 soil samples. Axes 1 and 2 are shown in the figure; Axis 3 accounts for 8.76% of the variation in community dissimilarities.

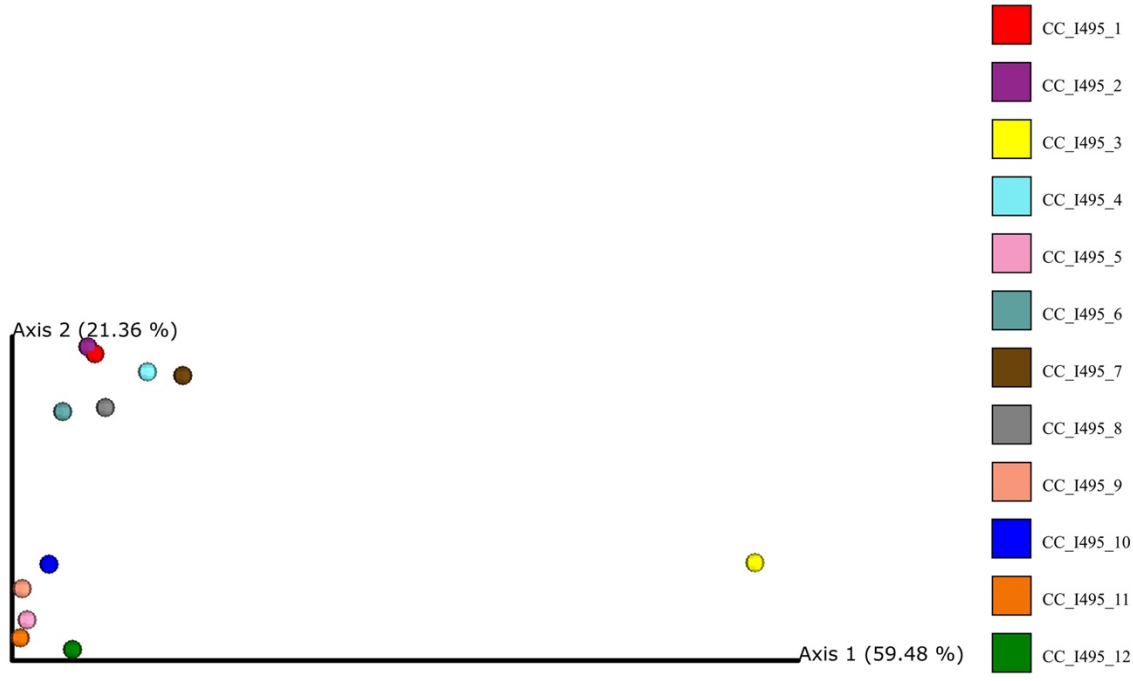

Figure 5. PCoA based on Weighted UniFrac distances, integrating both taxon abundance and phylogenetic relationships across 12 soil samples. Axes 1 and 2 are shown in the figure; Axis 3 accounts for 6.62% of the variation in community dissimilarities.

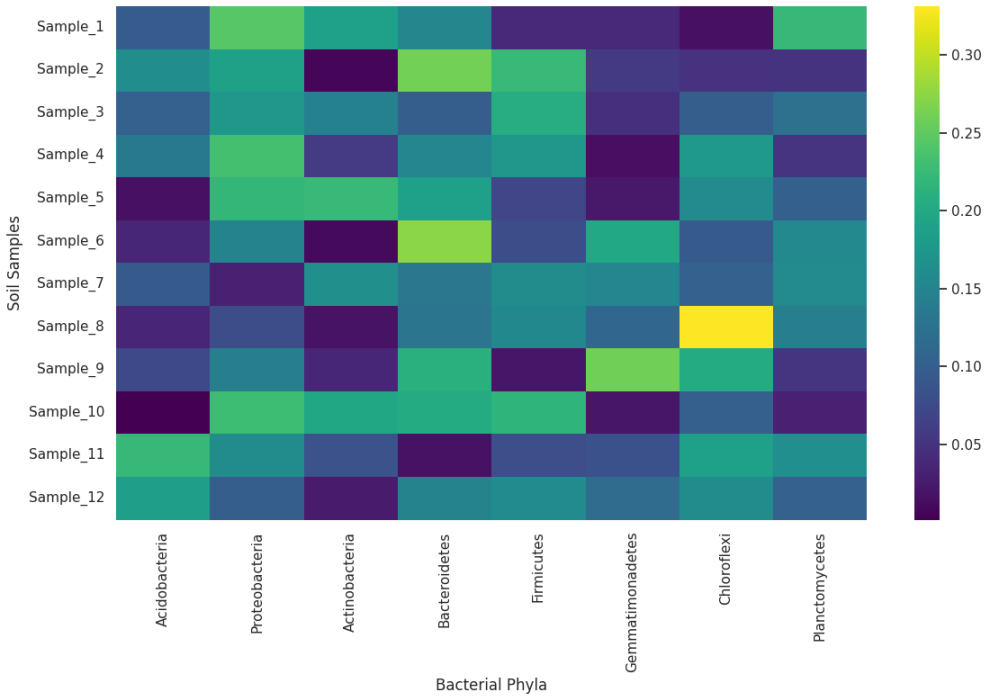

Figure 6. Heatmap displaying normalized relative abundance of eight representative taxa across 12 soil samples.

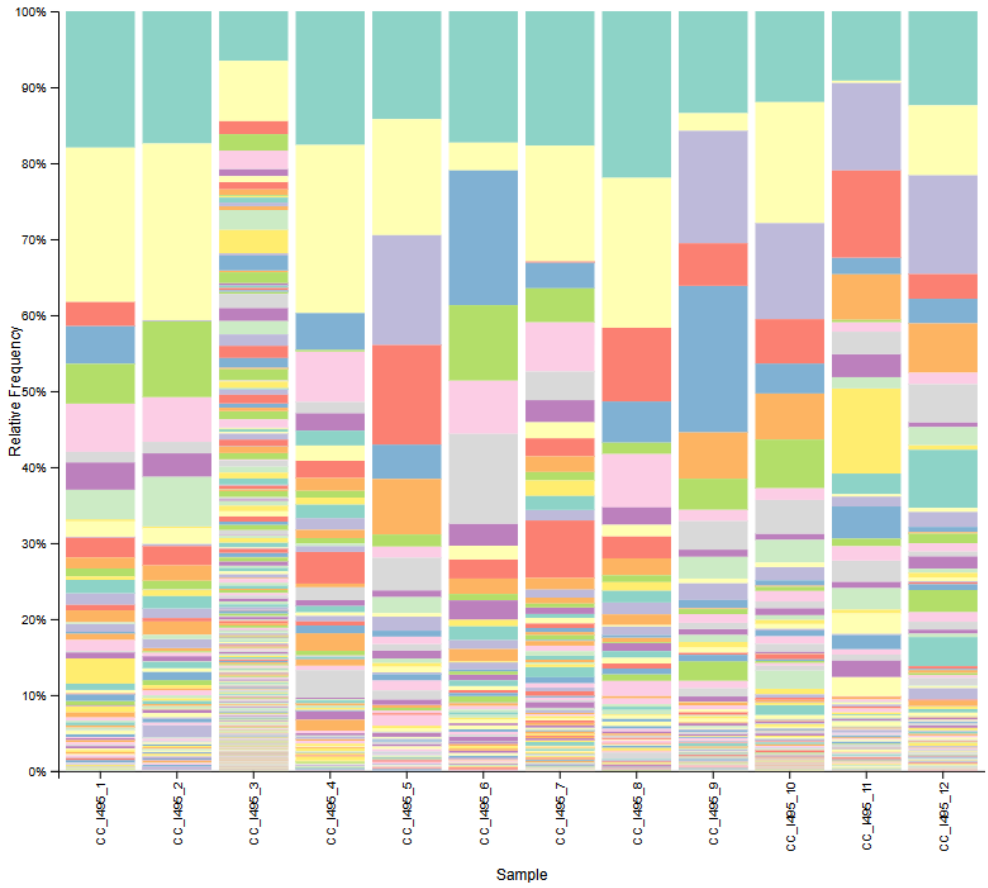

Figure 7. Visualization of operational taxonomic units (OTUs) at the species level. A total of 502 OTUs were identified. The complete color-coded legend associated with this figure is provided in Supplementary Material 2.

and *Achromobacter*. CC_I495_3 again stood out due to its high abundance of *Myxococcus* and *Nitrospira*, contributing to its unique placement. CC_I495_5 and CC_I495_8 remained outliers, reinforcing their distinct abundance and phylogenetic profiles. This metric effectively captured nuanced shifts in community structure, balancing the influence of dominant taxa with evolutionary relationships.

The heatmap (Figure 6) revealed distinct phylum-level shifts in microbial composition across the 12 soil samples. Samples CC_I495_1 and CC_I495_2, located closest to the roadside and at higher elevation, were dominated by Proteobacteria and Firmicutes, with reduced representation of Acidobacteria and Planctomycetes. These samples also corresponded to lower Shannon diversity and Faith's PD, suggesting taxonomic skew and limited phylogenetic breadth. In contrast, samples CC_I495_10 through CC_I495_12, furthest and highest from the roadside, exhibited more balanced phylum distributions, with increased abundance of Acidobacteria, Chloroflexi, and Gemmatimonadetes. These samples aligned with higher alpha diversity metrics, indicating more even and phylogenetically diverse communities. Sample CC_I495_3 stood out with elevated Actinobacteria and Planctomycetes, despite its proximity, but at an elevation match with the roadside, suggesting a unique ecological niche possibly buffered by microhabitat factors favoring dominance by stress-tolerant taxa.

Most Abundant OTUs

The microbial species, as well as the species abundance, greatly varied across the sampled sites. 199 OTUs were present across all the sampling locations while 114 OTUs unique to the NO-RC samples and 189 OTUs were unique to the RC samples (Figure 7).

Firmicutes, Proteobacteria and Actinobacteria dominated the phyla in the samples (Figure 8).

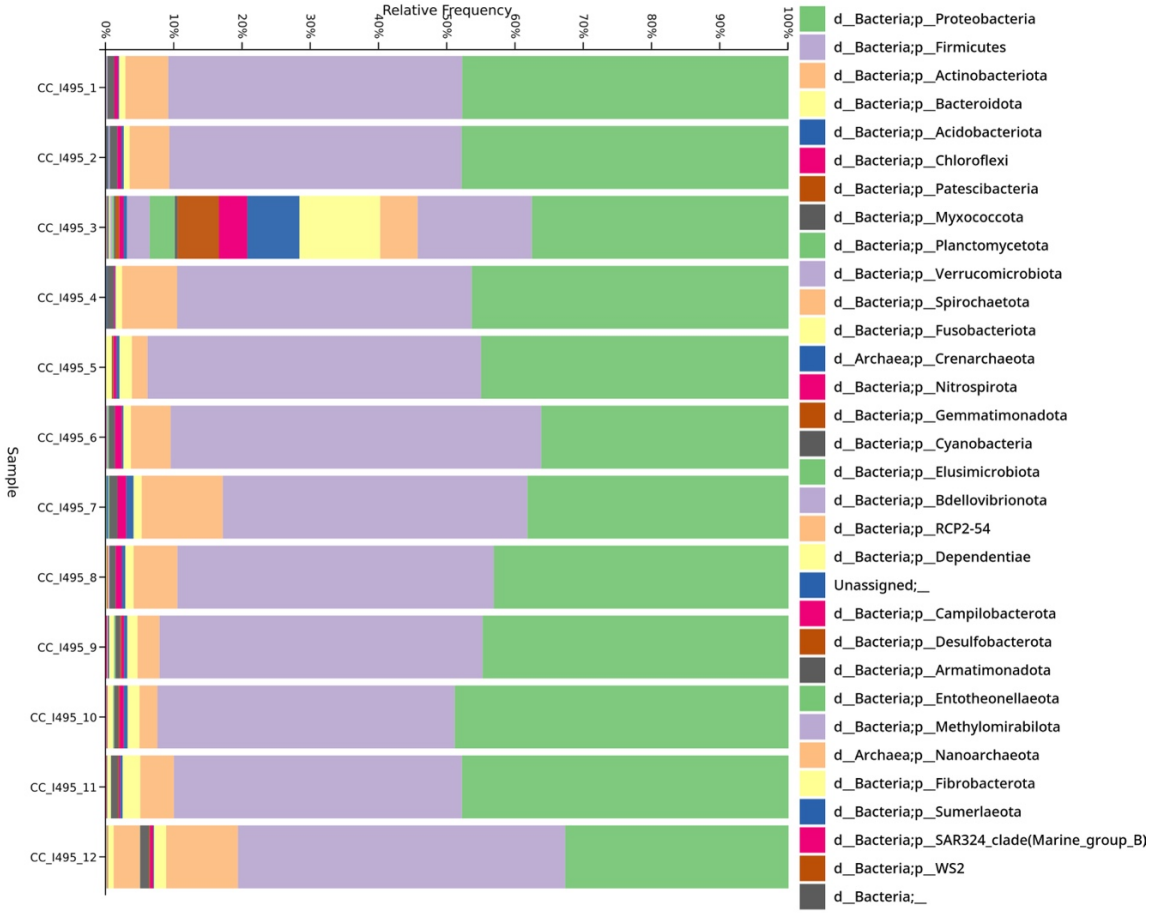

Figure 8. Visualization of OTUs at the phylum level. A total of 32 OTUs were identified.

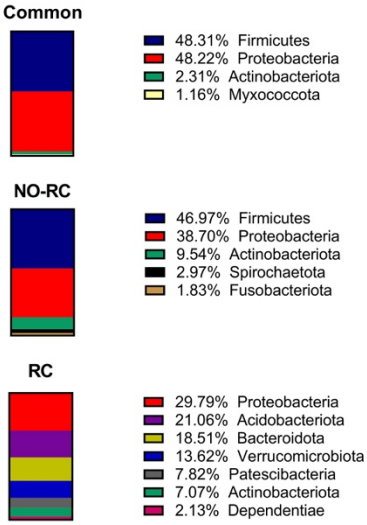

Figure 9. Average percent composition of phylum's composing the top 21 common OTUs (top), OTUs unique to soil samples with no RC (middle), and OTUs unique to soil samples with RC (bottom).

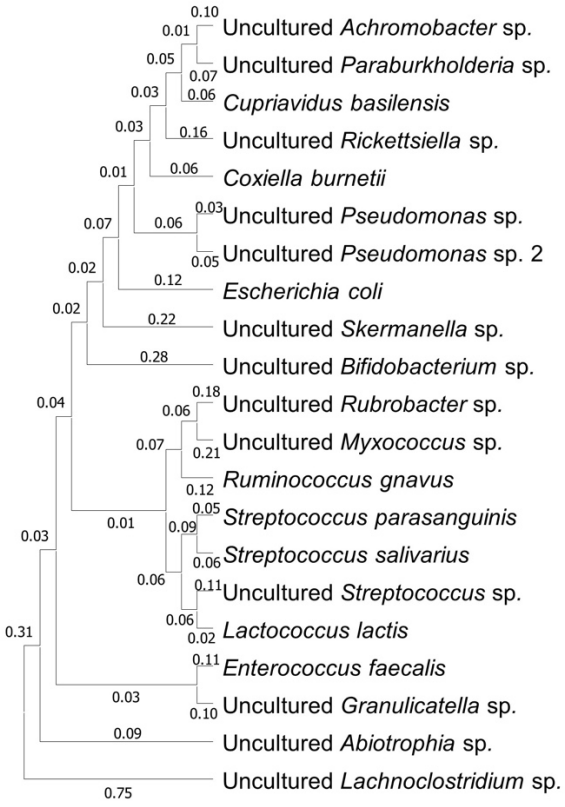

Figure 10. Dendrogram comparing the 16S rRNA gene V3/V4 region of the 21 most common OTUs located in both RC and NO-RC samples. All sequences were 301 bp. Numbers next to branches represent evolutionary distances, expressed as the number of base substitutions per site.

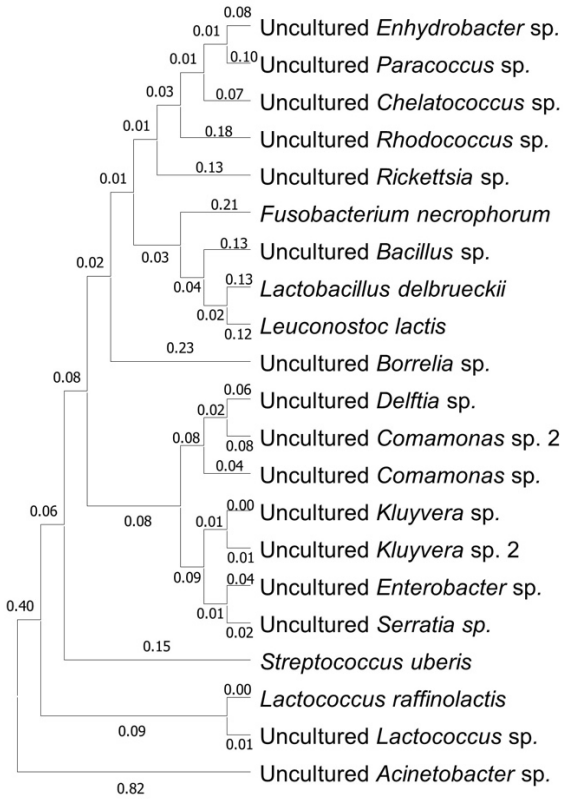

Figure 11. Dendrogram comparing the 16S rRNA gene V3/V4 region of the top 21 OTUs from NO-RC samples. All sequences were 301 bp. Numbers next to branches represent evolutionary distances, expressed as the number of base substitutions per site.

The top 21 OTUs common in all the samples were primarily from the phyla Firmicutes and Proteobacteria, with a small portion being Actinobacteriota and Myxococcota (Figure 9). The identified species included *Streptococcus parasanguinis, Streptococcus salivarius, Lactococcus lactis, Enterococcus faecalis, Ruminococcus gnavus, Coxiella burnetii, Escherichia coli* and *Cupriavidus basilensis*. There were also 13 uncultured species identified from the genera *Streptococcus, Abiotrophia, Lachnoclostridium, Granulicatella, Pseudomonas, Rickettsiella, Achromobacter, Paraburkholderia, Skermanella, Bifidobacterium, Rubrobacter* and *Myxococcus* (Figure 10). Many of these microorganisms are consistent across all the samples, including different proximities from the RC. The uncultured *Streptococcus* sp. showed in lower concentration in the RC samples, while *Streptococcus salivarius* was higher, when compared to the NO-RC samples.

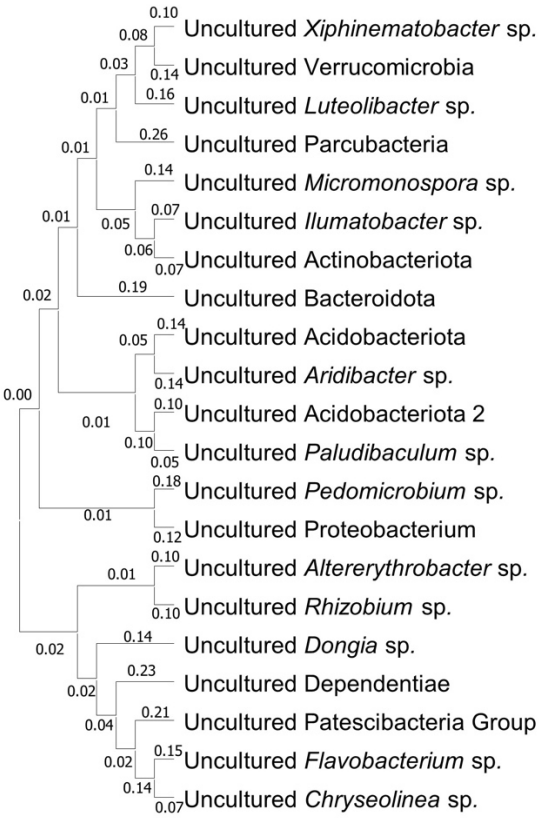

Figure 12. Dendrogram comparing the 16S rRNA gene V3/V4 region of the top 21 OTUs from samples exposed to RC. All sequences were 301 bp. Numbers next to branches represent evolutionary distances, expressed as the number of base substitutions per site.

The top 21 average NO-RC OTUs were also primarily from the phyla Firmicutes and Proteobacteria; however, the samples had higher proportions of Actinobacteriota than the common OTUs while also showing a considerable portion of Spirochaetota and Fusobacteriota (Figure 8). The identified species included *Streptococcus uberis, Lactococcus raffinolactis, Lactobacillus delbrueckii, Leuconostoc lactis* and *Fusobacterium necrophorum*. There were also 16 uncultured species from the genera *Lactococcus, Bacillus, Kluyvera, Enhydrobacter, Delftia, Chelatococcus, Paracoccus, Comamonas, Rickettsia, Enterobacter, Acinetobacter, Serratia, Rhodococcus and Borrelia* (Figure 11). The abundance of the NO-RC OTUs was not consistent across all the samples from varying proximities to Interstate-495. *Delftia* and *Paracoccus* did not show in samples 4-6, *Lactococcus raffinolactis*, *Delftia* and *Chelatococcus* did not show in samples 7-9, and the uncultured *Acinetobacter* did not show in samples 10-12.

The top 21 RC OTUs showed the greatest diversity of phyla containing Proteobacteria, Verrucomicrobiota, Bacteroidota, Acidobacteriota, Patescibacteria, Actinobacteriota and Dependentiae (Figure 8). All 21 OTUs were uncultured species belonging to the genera *Dongia*, *Altererythrobacter*, *Pedomicrobium*, *Rhizobium*, *Luteolibacter*, *Xiphinematobacter*, *Flavobacterium*, *Chryseolinea*, *Paludibaculum*, *Aridibacter*, *Ilumatobacter*, and *Micromonospora*, as well as taxa assigned to the phyla Verrucomicrobiota, Bacteroidota, and Acidobacteriota, and to candidate phyla within the Patescibacteria superphylum (including Parcubacteria). Five additional OTUs were classified only at the phylum level as members of Proteobacteria, Acidobacteriota, Actinobacteriota, and Dependentiae (Figure 12). The bacteria comprising the top 21 most abundant RC OTUs showed in similar amounts, and all 21 of the OTUs stemmed from sample 3.

DISCUSSION

Spatial and Elevation Gradients in Microbial Community Structure

The beta diversity analyses revealed clear spatial and elevation structuring of microbial communities across the 12 soil samples. Samples CC_I495_1 and CC_I495_2, located closest to the roadside and at a higher elevation, exhibited reduced Shannon diversity and lower Faith's Phylogenetic Diversity. These samples were dominated by *Coxiella burnetii*, *Streptococcus* spp., and *Achromobacter*, suggesting environmental stress or anthropogenic influence associated with roadside proximity and elevation. Notably, CC_I495_3, despite sharing elevation with the roadside, displayed a remarkably high Shannon index (7.67) and Faith's PD (27.14), indicating a uniquely resilient and phylogenetically rich community. Its distinct placement across all beta diversity metrics suggests that elevation to RC plays a role in microbial structure.

Samples CC_I495_4 through CC_I495_12, located progressively farther and higher from the roadside, demonstrated a gradient of increasing diversity and phylogenetic breadth. The furthest samples (CC_I495_10–CC_I495_12) clustered tightly in Bray-Curtis and Weighted UniFrac plots, with elevated diversity indices and broader representation of taxa such as *Pseudomonas*, *Streptococcus parasanguinis*, and *Enterococcus faecalis*. Intermediate samples (CC_I495_4–

CC_I495_9) showed transitional profiles, with gradual shifts in both taxonomic composition and evolutionary structure.

Samples CC_I495_3 and CC_I495_7 exhibited the highest Shannon Diversity Index (7.67 and 5.07, respectively) and Faith's Phylogenetic Diversity (27.14 and 11.80), corresponding with broad representation of taxa such as *Coxiella burnetii*, *Streptococcus parasanguinis*, *Pseudomonas*, *Myxococcus*, and *Nitrospira*. These samples displayed balanced abundance profiles and high evenness, suggesting a stable and phylogenetically rich microbial community. In contrast, samples CC_I495_5 and CC_I495_8 showed reduced diversity and evenness, with dominance of fewer taxa including *Rubrobacter*, *Leuconostoc lactis*, and *Achromobacter*. These skewed profiles indicate potential niche specialization or environmental stress. Intermediate samples (e.g., CC_I495_10, CC_I495_11, CC_I495_12) maintained moderate diversity and shared several core taxa with the high-diversity cluster, though with less phylogenetic breadth.

Metric-Specific Insights

Bray-Curtis and Weighted UniFrac metrics captured abundance-driven shifts, emphasizing the influence of roadside proximity and elevation on dominant taxa. Jaccard and Unweighted UniFrac metrics revealed turnover in community membership and phylogenetic novelty, particularly in samples CC_I495_5 and CC_I495_8, which harbored rare taxa such as *Rubrobacter*, *Leuconostoc lactis*, and *Bifidobacterium*. These outliers may reflect microhabitat specialization or stochastic colonization events at intermediate elevations.

The consistent separation of CC_I495_3 across all metrics, despite its roadside elevation, suggests a unique ecological niche. Its elevated diversity and presence of evolutionarily distinct taxa (*Myxococcus*, *Nitrospira*) point to potential buffering mechanisms, such as localized vegetation or soil heterogeneity, that mitigate the expected impact of elevation and proximity.

Common OTUs

Many OTUs shared between RC and NO-RC soils represent ubiquitous soil symbionts, including *Lactococcus lactis*, *Escherichia coli*, *Streptococcus parasanguinis*, *Pseudomonas* and *Bifidobacterium* (Baty *et al.*, 2022; Mehmood *et al.*, 2023). *Achromobacter*, *Rubrobacter*, and *Cupriavidus basilensis* are adapted to salinity and heavy-metal stress (Kugler *et al.*, 2022). Other common OTUs reflect typical soil ecological roles such as *Myxococcus* in plant-rich detritus (Dawid, 2000), *Rickettsiella* in arthropod-associated niches (Jurat-Fuentes & Jackson, 2012), and *Coxiella burnetii* introduced through livestock waste (Abeykoon *et al.*, 2021). Several gastrointestinal-associated genera (e.g., *Ruminococcus, Enterococcus, Lachnoclostridium*) likely originate from wildlife or domestic animals (Byappanahalli *et al.*, 2012).

NO-RC OTUs

NO-RC soils contained numerous plant growth promoting bacteria, including *Rhizobacteria, Bacillus, Acinetobacter, Serratia,* and *Enterobacter*, which contribute to nutrient solubilization, phytohormone production, and stress reduction (Ji *et al.*, 2020; Mujumdar *et al.*, 2023; Saxena *et al.*, 2020). Genera such as *Chelatococcus* and *Enhydrobacter* participate in organic matter turnover (Li *et al.*, 2023; Premalatha *et al.*, 2015). Several taxa also support bioremediation, including *Rhodococcus, Comamonas*, *Delftia*, and *Paracoccus*, which degrade xenobiotics or detoxify metals (Hussein *et al.*, 2024; Martínková *et al.*, 2009). Additional OTUs reflected inputs from arthropods (*Borrelia, Rickettsia*) or livestock-associated environments (*Fusobacterium necrophorum, Rhodococcus*) (Ayoade F, 2024; Heise *et al.*, 2014).

RC OTUs

RC soils contained OTUs associated with pollution-tolerant or metal-resistant taxa, including members of the phyla Verrucomicrobiota, Actinobacteriota, and Acidobacteriota, as well as the genus *Flavobacterium* (Kou *et al.*, 2023; Nixon *et al.*, 2019). The genera *Micromonospora* and *Ilumatobacter*, and taxa within the phylum Dependentiae, encode metallophore production and metal-resistance pathways (Liu *et al.*, 2022). Additional RC-specific taxa such as *Pedomicrobium, Altererythrobacter*, and *Dongia* are commonly enriched in metal-contaminated or mining-adjacent soils (Gao *et al.*, 2025; Ren *et al.*, 2021). Nitrogen-cycling taxa included the genus *Aridibacter* and candidate phyla within the Patescibacteria superphylum, while carbohydrate-degrading groups included the genus *Chryseolinea* and the candidate

phylum Parcubacteria (Herrmann *et al.*, 2019; Liang *et al.*, 2023). The presence of Bacteroidota exclusively in RC soils may reflect sensitivity to fertilizers commonly used in cemetery landscaping (Ali *et al.*, 2024).

Implications

Microbial patterns across Calvary Cemetery align with known effects of roadside pollution, soil compaction, and altered moisture regimes (De Silva *et al.*, 2021). Elevation modulated these impacts: the sample at equal elevation to the roadway exhibited the highest richness and phylogenetic diversity, consistent with studies showing that vertical gradients influence microbial assembly near highways (Liu *et al.*, 2021). Higher-elevation soils supported more functionally diverse communities, whereas low-elevation RC soils showed reduced diversity and greater dominance by stress-tolerant taxa.

These findings highlight the need to consider both distance and elevation when assessing microbial responses to roadside environments. Incorporating soil chemistry and functional metagenomics would clarify mechanisms underlying these patterns and help identify taxa with bioremediation potential. Given the global extent of high-traffic highways (Federation, 2023), roadside soils represent a substantial reservoir of microbial diversity with relevance for pollution mitigation and ecological restoration.

CONCLUSION

In conclusion, soil exposed to RC did show to have a different bacteria composition as compared to soil with NO-RC. Most of the NO-RC specific OTUs were plant growth promoting bacteria, as well as bacteria that facilitate the breakdown of organic material. There was a smaller precedence of bacteria known to remediate heavy metals or polyaromatic hydrocarbons (PAHs) in the NO-RC sample group, but they were present. Most of the RC OTUs were bacteria linked to various heavy metals or PAHs, both for their persistence-in and remediation-of heavy metals. As expected, the OTUs found ubiquitously across the entire sampling area were hallmark bacteria known to be found across different types of soil and environmental conditions.

ACKNOWLEDGEMENTS

Igor Ivanovski acknowledges support from the SJNY Faculty Small Grant and the SJNY Summer Grant.

AUTHOR CONTRIBUTIONS

Igor Ivanovski: Conceptualization (lead); funding acquisition (lead); writing – original draft (lead); formal analysis (lead); writing – review and editing (lead). Catalina Garcia Canas: Writing – original draft (supporting); formal analysis (supporting). Ghazwan Qasim Hasan: Formal analysis (supporting).

DATA AVAILABILITY STATEMENT

The raw sequencing data supporting the conclusions of this article are available in the NCBI SRA under accession number PRJNA1248142.

CONFLICT OF INTEREST

None declared.

REFERENCES

Abeykoon, A. H., Clark, N. J., Soares Magalhaes, R. J., Vincent, G. A., Stevenson, M. A., Firestone, S. M., & Wiethoelter, A. K. (2021). *Coxiella burnetii* in the environment: A systematic review and critical appraisal of sampling methods. Zoonoses and Public Health, 68(3), 165-181. DOI: 10.1111/zph.12791

Ali, N., Jiang, Q., Luo, R., Jiang, M., Wang, X., Akhtar, K., He, B., & Wen, R. (2024). Foliar application of bioorganic fertilizer enhances plant nutrients uptake and citrus yield by regulating rhizosphere and phyllosphere microbiome. Environmental Technology & Innovation, 36, 103902. DOI: 10.1016/j.eti.2023.103902

Anigilaje, E. A., Nasir, Z. A., & Walton, C. (2024). Exposure to benzene, toluene, ethylbenzene, and xylene (BTEX) at Nigeria's petrol stations: a review of current status, challenges and future directions. Frontiers in Public Health, 12, 1295758. DOI: 10.3389/fpubh.2024.1295758

Atlas, R. M. (1981). Microbial degradation of petroleum hydrocarbons: an environmental perspective. Microbiology Reviews, 45(1), 180-209. DOI: 10.1128/mr.45.1.180-209.1981

Ayoade F, V. S., Alam MU. (2024). Rhodococcus Equi. In: StatPearls [Internet]. Treasure Island (FL): StatPearls Publishing. Available from https://www.ncbi.nlm.nih.gov/books/NBK441978/

Baty, J. J., Huffines, J. T., Stoner, S. N., & Scoffield, J. A. (2022). A Commensal *Streptococcus* dysregulates the *Pseudomonas aeruginosa* nitrosative stress response.

Frontiers in Cellular and Infection Microbiology, 12, 817336. DOI: 10.3389/fcimb.2022.817336

bcl-convert. A proprietary Illumina software for the conversion of bcl files to basecalls. https://supportdocs.illumina.com/SW/BCL_Convert/Content/SW/BCLConvert/Introduction_swBCL.htm

Benjamin J Callahan, Paul J McMurdie, Michael J Rosen, Andrew W Han, Amy Jo A Johnson, & Holmes, S. P. (2016). Dada2: high-resolution sample inference from illumina amplicon data. Nature Methods, 13(7), 581. DOI: 10.1038/nmeth.3869.

Bessagnet, B., Allemand, N., Putaud, J. P., Couvidat, F., André, J. M., Simpson, D., Pisoni, E., Murphy, B. N., & Thunis, P. (2022). Emissions of carbonaceous particulate matter and ultrafine particles from vehicles-a scientific review in a cross-cutting context of air pollution and climate change. Applied Sciences, 12(7), 1-52. DOI: 10.3390/app12073623

Bolyen, E., Rideout, J.R., Dillon, M.R. (2019). Reproducible, interactive, scalable and extensible microbiome data science using QIIME 2. Nature Biotechnology, 37, 852-857. DOI: 10.1038/s41587-019-02099

Byappanahalli, M. N., Nevers, M. B., Korajkic, A., Staley, Z. R., & Harwood, V. J. (2012). Enterococci in the environment. Microbiology and Molecular Biology Reviews: MMBR, 76(4), 685-706. DOI: 10.1128/mmbr.00023-12

Caputo, D., Rattansingh, J., Hernandez, V., & Nash, B. (2019). An analysis of soil microhabitats in Revolutionary War, Civil War, and modern graveyards on Long Island, NY. Journal of Emerging Investigators, 2(1), 1-5. DOI: 10.59720/18-017

Dawid, W. (2000). Biology and global distribution of myxobacteria in soils. FEMS Microbiology Reviews, 24(4), 403-427. DOI: 10.1111/j.1574-6976.2000.tb00548.x

De Silva, S., Ball, A. S., Shahsavari, E., Indrapala, D. V., & Reichman, S. M. (2021). The effects of vehicular emissions on the activity and diversity of the roadside soil microbial community. Environmental Pollution, 277, 116744. DOI: 10.1016/j.envpol.2021.116744

Federation, I. R. (2023). World Road Statistics 2023 https://vividmaps.com/worlds-roads/

Gao, W., Chen, S., Yu, X., Chen, S., Wan, C., Wang, Y., Wu, P., & Li, Q. (2025). Three local plants adapt to ecological restoration of abandoned lead-zinc mines through assembly of rhizosphere bacterial communities. Frontiers in Microbiology, 16, 1533965. DOI: 10.3389/fmicb.2025.1533965

He, Y., Xu, Y., Lv, Y., Nie, L., & Wang, H. (2020). Soil bacterial community structure in turfy swamp and its response to highway disturbance. International Journal of Environmental Research and Public Health, 17(21), 7822. DOI: 10.3390/ijerph17217822

Heise, S. R., Elshahed, M., & Little, S. (2014). Bacterial diversity in *Amblyomma americanum* (Acari: Ixodidae) with a focus on members of the genus *Rickettsia*. Journal of Medical Entomology, 47(2), 258-268. DOI: 10.1603/ME13164

Herrmann, M., Wegner, C.-E., Taubert, M., Geesink, P., Lehmann, K., Yan, L., Lehmann, R., Totsche, K. U., & Küsel, K. (2019). Predominance of Cand. Patescibacteria in groundwater is caused by their preferential mobilization from soils and flourishing under oligotrophic conditions. Frontiers in Microbiology, 10, 1407. DOI: 10.3389/fmicb.2019.01407

Hussein, S. H., Qurbani, K., Ahmed, S. K., Tawfeeq, W., & Hassan, M. (2024). Bioremediation of heavy metals in contaminated environments using *Comamonas* species: A narrative review. Bioresource Technology Reports, 25, 101711. DOI: 10.1016/j.biteb.2023.101711

Ji, C., Liu, Z., Hao, L., Song, X., Wang, C., Liu, Y., Li, H., Li, C., Gao, Q., & Liu, X. (2020). Effects of *Enterobacter cloacae* HG-1 on the nitrogen-fixing community structure of wheat rhizosphere soil and on salt tolerance. Frontiers in Plant Science, 11, 1094. DOI: 10.3389/fpls.2020.01094

Jurat-Fuentes, J. L., & Jackson, T. A. (2012). Bacterial entomopathogens. Insect Pathology, 265-349. DOI: 10.1016/B978-0-12-384984-7.00008-7

Kaur, J., Bhat, S. A., Singh, N., Bhatti, S. S., Kaur, V., & Katnoria, J. K. (2022). Assessment of the heavy metal contamination of roadside soils alongside Buddha Nullah, Ludhiana, (Punjab) India. International Journal of Environmental Research and Public Health, 19(3), 1596. DOI: 10.3390/ijerph19031596

Kou, B., He, Y., Wang, Y., Qu, C., Tang, J., Wu, Y., Tan, W., Yuan, Y., & Yu, T. (2023). The relationships between heavy metals and bacterial communities in a coal gangue site. Environmental Pollution, 322, 121136. DOI: 10.1016/j.envpol.2023.121136

Kugler, A., Brigmon, R. L., Friedman, A., Coutelot, F. M., Polson, S. W., Seaman, J. C., & Simpson, W. (2022). Bioremediation of copper in sediments from a constructed wetland ex situ with the novel bacterium *Cupriavidus basilensis* SRS. Scientific Reports, 12(1), 17615. DOI: 10.1038/s41598-022-20930-0

Larkin, M. A., Blackshields, G., Brown, N. P., Chenna, R., McGettigan, P. A., McWilliam, H., Valentin, F., Wallace, I. M., Wilm, A., Lopez, R., Thompson, J. D., Gibson, T. J., & Higgins, D. G. (2007). Clustal W and Clustal X version 2.0. Bioinformatics, 23(21), 2947-2948. DOI: 10.1093/bioinformatics/btm404

Leahy, J. G., & Colwell, R. R. (1990). Microbial degradation of hydrocarbons in the environment.

Microbiology Reviews, 54(3), 305-315. DOI: 10.1128/mr.54.3.305-315.1990

Li, T., Zhang, X., Wang, X., Yan, Z., Peng, C., Zhao, S., Xu, D., Liu, D., & Shen, Q. (2023). Effect of inoculating thermophilic bacterial consortia on compost efficiency and quality. Waste Management, 170, 341-353. DOI: 10.1016/j.wasman.2023.07.021

Li, Y. Q., Xin, Y., Li, C., Liu, J., & Huang, T. (2023). Metagenomics-metabolomics analysis of microbial function and metabolism in petroleum-contaminated soil. Brazilian Journal of Microbiology, 54(2), 935-947. DOI: 10.1007/s42770-023-01000-7

Liang, Y., Yin, Q., Jiang, Z., Yan, H., & Nian, Y. (2023). Pollution characteristics and microbial community succession of a rural informal landfill in an arid climate. Ecotoxicology and Environmental Safety, 262, 115295. DOI: 10.1016/j.ecoenv.2023.115295

Liu, Y., Gao, T., Wang, X., Fu, J., Zuo, M., Yang, Y., Yin, Z., Wang, Z., Tai, X., & Chang, G. (2022). Effects of heavy metals on bacterial community surrounding Bijiashan mining area located in northwest China. Open Life Sciences, 17(1), 40-54. DOI: 10.1515/biol-2022-0008

Liu, Z., Yang, Y., Ji, S., Dong, D., Li, Y., Wang, M., Han, L., & Chen, X. (2021). Effects of elevation and distance from highway on the abundance and community structure of bacteria in soil along Qinghai-Tibet Highway. International Journal of Environmental Research and Public Health, 18(24), 13137. DOI: 10.3390/ijerph182413137

Lotfalian, M., & Nasiri, M. (2018). The distribution and frequency of damage to roadside trees in low-volume road construction. Journal of Forestry Research, 29(1), 221-226. DOI: 10.1007/s11676-017-0433-4

Martin, M. (2011). Cutadapt removes adapter sequences from high-throughput sequencing reads. EMBnet.Journal, 17(1), 1-10. DOI: 10.14806/ej.17.1.200

Martínková, L., Uhnáková, B., Pátek, M., Nešvera, J., & Křen, V. (2009). Biodegradation potential of the genus *Rhodococcus*. Environment International, 35(1), 162-177. DOI: 10.1016/j.envint.2008.07.018

Mehmood, N., Saeed, M., Zafarullah, S., Hyder, S., Rizvi, Z. F., Gondal, A. S., Jamil, N., Iqbal, R., Ali, B., & Ercisli, S. (2023). Multifaceted impacts of plant-beneficial *Pseudomonas* spp. in managing various plant diseases and crop yield improvement. ACS Omega, 8(25), 22296-22315. DOI: 10.1021/acsomega.3c00870

Melekhina, E. N., Belykh, E. S., Markarova, M. Y., Taskaeva, A. A., Rasova, E. E., Baturina, O. A., Kabilov, M. R., & Velegzhaninov, I. O. (2021). Soil microbiota and microarthropod communities in oil contaminated sites in the European Subarctic. Scientific Reports, 11(1), 19620. DOI: 10.1038/s41598-021-98680-8

Mujumdar, S., Bhoyar, J., Akkar, A., Hundekar, S., Agnihotri, N., Jaybhay, P., & Bhuyan, S. (2023). *Acinetobacter*: A versatile plant growth-promoting rhizobacteria (PGPR). In: Plant-microbe interaction-recent advances in molecular and biochemical approaches (pp. 327-362). Elsevier. DOI: 10.1016/B978-0-323-90527-1.00017-4

Nixon, S. L., Daly, R. A., Borton, M. A., Solden, L. M., Welch, S. A., Cole, D. R., Mouser, P. J., Wilkins, M. J., & Wrighton, K. C. (2019). Genome-resolved metagenomics extends the environmental distribution of the Verrucomicrobia phylum to the deep terrestrial subsurface. Msphere, 4(6), 00613-00619. DOI: 10.1128/mSphere.00613-19

Premalatha, N., Gopal, N. O., Jose, P. A., Anandham, R., & Kwon, S.-W. (2015). Optimization of cellulase production by *Enhydrobacter* sp. ACCA2 and its application in biomass saccharification. Frontiers in Microbiology, 6, 1046. DOI: 10.3389/fmicb.2015.01046

Ren, C., Teng, Y., Chen, X., Shen, Y., Xiao, H., & Wang, H. (2021). Impacts of earthworm introduction and cadmium on microbial communities composition and function in soil. Environmental Toxicology and Pharmacology, 83, 103606. DOI: 10.1016/j.etap.2021.103606

Saitou, N., & Nei, M. (1987). The neighbor-joining method: a new method for reconstructing phylogenetic trees. Molecular Biology & Evolution, 4(4), 406-425. DOI: 10.1093/oxfordjournals.molbev.a040454

Saxena, A. K., Kumar, M., Chakdar, H., Anuroopa, N., & Bagyaraj, D. (2020). *Bacillus* species in soil as a natural resource for plant health and nutrition. Journal of Applied Microbiology, 128(6), 1583-1594. DOI: 10.1111/jam.14506

Singh, S., & Hiranmai, R. Y. (2021). Monitoring and molecular characterization of bacterial species in heavy metals contaminated roadside soil of selected region along NH 8A, Gujarat. Heliyon, 7(11), e08284. DOI: 10.1016/j.heliyon.2021.e08284

Tamura, K., Nei, M., & Kumar, S. (2004). Prospects for inferring very large phylogenies by using the neighbor-joining method. Proceedings of the National Academy of Sciences of the United States of America, 101(30), 11030-11035. DOI: 10.1073/pnas.0404206101

Tamura, K., Stecher, G., & Kumar, S. (2021). MEGA11: Molecular Evolutionary Genetics Analysis Version 11. Molecular Biology & Evolution, 38(7), 3022-3027. DOI: 10.1093/molbev/msab120

Torbjørn Rognes, Tomáš Flouri, Ben Nichols, Christopher Quince, & Mahé, a. F. (2016). Vsearch: a versatile open source tool for metagenomics. Peer J, 4, e2584. DOI: 10.7717/peerj.2584

Transportation, N. Y. S. D. o. (2019). Draft Design Report for Project 022948. https://www.dot.ny.gov/portal/page/portal/content/delivery/region10/projects/022948-Home/022948-Repository/0229.48_RPT_DDR_Draft%20Design%20Report_12-6-19.pdf

Yang, H.-H., Dhital, N. B., Wang, L.-C., Hsieh, Y.-S., Lee, K.-T., Hsu, Y.-T., & Huang, S.-C. (2019). Chemical characterization of fine particulate matter in gasoline and diesel vehicle exhaust. Aerosol and Air Quality Research, 19(6), 1439-1449. DOI: 10.4209/aaqr.2019.04.0191

Žibret, G., Van Tonder, D., & Žibret, L. (2013). Metal content in street dust as a reflection of atmospheric dust emissions from coal power plants, metal smelters, and traffic. Environmental Science and Pollution Research International, 20(7), 4455-4468. DOI: 10.1007/s11356-012-1398-7

Submitted: 19 April 2026

First decision: 14 August 2026

Accepted: 20 August 2026

Published online: 8 September 2026

Edited by Thorsten Lumbsch